

# Statistical Optimization of Adsorption of a Harmful Dye from Aqueous Solution

M. Arun, A. Kannan

## I. INTRODUCTION

**Abstract**—Textile industries cater to varied customer preferences and contribute substantially to the economy. However, these textile industries also produce a considerable amount of effluents. Prominent among these are the azo dyes which impart considerable color and toxicity even at low concentrations. Azo dyes are also used as coloring agents in food and pharmaceutical industry. Despite their applications, azo dyes are also notorious pollutants and carcinogens. Popular techniques like photo-degradation, biodegradation and the use of oxidizing agents are not applicable for all kinds of dyes, as most of them are stable to these techniques. Chemical coagulation produces a large amount of toxic sludge which is undesirable and is also ineffective towards a number of dyes. Most of the azo dyes are stable to UV-visible light irradiation and may even resist aerobic degradation. Adsorption has been the most preferred technique owing to its less cost, high capacity and process efficiency and the possibility of regenerating and recycling the adsorbent. Adsorption is also most preferred because it may produce high quality of the treated effluent and it is able to remove different kinds of dyes. However, the adsorption process is influenced by many variables whose interdependence makes it difficult to identify optimum conditions. The variables include stirring speed, temperature, initial concentration and adsorbent dosage. Further, the internal diffusional resistance inside the adsorbent particle leads to slow uptake of the solute within the adsorbent. Hence, it is necessary to identify optimum conditions that lead to high capacity and uptake rate of these pollutants. In this work, commercially available activated carbon was chosen as the adsorbent owing to its high surface area. A typical azo dye found in textile effluent waters, viz. the monoazo Acid Orange 10 dye (CAS: 1936-15-8) has been chosen as the representative pollutant. Adsorption studies were mainly focused at obtaining equilibrium and kinetic data for the batch adsorption process at different process conditions. Studies were conducted at different stirring speed, temperature, adsorbent dosage and initial dye concentration settings. The Full Factorial Design was the chosen statistical design framework for carrying out the experiments and identifying the important factors and their interactions. The optimum conditions identified from the experimental model were validated with actual experiments at the recommended settings. The equilibrium and kinetic data obtained were fitted to different models and the model parameters were estimated. This gives more details about the nature of adsorption taking place. Critical data required to design batch adsorption systems for removal of Acid Orange 10 dye and identification of factors that critically influence the separation efficiency are the key outcomes from this research.

**Keywords**—Acid Orange 10, Activated carbon, Optimum conditions, Statistical design.

M. Arun is with the Department of Chemical Engineering, Indian Institute of Technology, Madras, Chennai, 600036, India (e-mail: arun.kumaran917@gmail.com).

A. Kannan is with the Department of Chemical Engineering, Indian Institute of Technology, Madras, Chennai, 600036, India (Corresponding author phone number: +91-044-2257 4170, e-mail: kannan@iitm.ac.in).

TEXTILE industry is one of the most important manufacturing sectors in the country. It contributes heavily to the GDP of the country and a lot of employment as well. There are a lot of skilled as well as unskilled laborers employed in this industry. Dyeing is one of the most important division in a textile industry. Because of the expansion in the textile industry the dyeing operations are also increasing. The dyeing industry takes up a lot of water. Water is used as a solvent in these industries. The water released after the dyeing process is let out into water bodies in turn polluting them. This not only affects aquatic life but gets carried through the food chain to other higher level organisms as well.

Azo dyes belong to one of the most important classes of dyes used in the textile industries. Apart from being used in dyeing industry they are also used in food and pharmaceutical industry as coloring agents [1]. Despite their applications azo dyes are highly toxic and are a cause of water pollution. Even at low concentrations they impart considerable color and toxicity. Widely used techniques such as photo-degradation, biodegradation and the use of oxidizing agents are not applicable for all types of dyes. Most of the dyes are stable to these techniques [2].

Adsorption is one of the most preferred technique. The reason for its wide spread use may be because it's less expensive, highly efficient and it is possible to recycle the adsorbent. The adsorption process is influenced by many process variables. Some of which are stirring speed, temperature, initial dye concentration and adsorbent loading. Therefore, it is essential to find out the optimal conditions which when applied will lead to maximum dye uptake from the solution.

Commercially available activated carbon was used as the adsorbent and Acid Orange 10 was chosen as the representative dye. The main focus of experimentation is to obtain Equilibrium and kinetic data which are crucial. Another important aspect of experimentation is to be able to perform the experiments in the most efficient and effective manner. Design of Experiments (DOE) is a tool that is being increasingly used for this purpose. The full factorial design was the chosen design framework for carrying out the experiments. The main aim is to understand the complex physio-chemical interactions between the dye molecules and the adsorbent. For this purpose, the characteristics of the carbon were investigated. Optimal conditions were obtained from the statistical model. Experiments were performed at these process conditions for validation.

## II. MATERIALS AND METHODS

## A. Adsorbate

Acid Orange 10 (AO10) dye was procured from Sisco Research Laboratories Pvt. Ltd. (Mumbai, India). The structure of AO10 and its characteristics is shown in Fig. 1 and Table I respectively. AO10 is a monoazo dye that comes as a disodium salt.

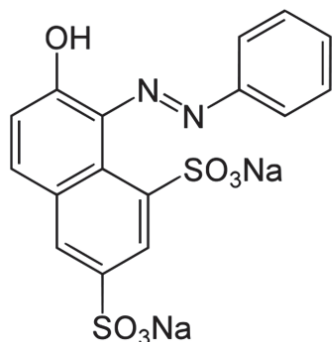


Fig. 1 Structure of Acid Orange 10

TABLE I  
PHYSICAL AND CHEMICAL CHARACTERISTICS OF ACID ORANGE 10

Chemical Name	Acid Orange 10
Color Index Number	16230
Abbreviation	AO10
Commercial Name	Orange G
Molecular formula	$C_{16}H_{10}N_2Na_2O_7S_2$
Molecular Structure	Single azo class
Molecular weight	452.37
$\lambda_{max}$ (nm)	477-478

## B. Adsorbent

Activated carbon (AC) was bought from Active Char Limited (Edayar, Kerala). Sieve analysis was performed with the AC. The average particle size selected for conducting the experiments was 0.4625 mm. After sieve analysis, the carbon was washed thoroughly with deionized water. It was washed until complete removal of any fines present. The AC was then dried in a hot air oven at 110°C for a period of 24 hours. The dried AC was then stored in a desiccator in order to avoid contact with moisture present in the air.

## C. Process Vessel

Process vessel was designed and fabricated to suit the experimental needs and to provide complete mixing of the contents. The interior wall of the process vessel was fitted with baffles in order to prevent vortex formation at high stirrer speeds and to facilitate proper mixing. The vessel was provided with a water jacket for the circulation of water to control the temperature of the process mixture. The inlet and outlet from the jacket were connected to a constant temperature bath for maintaining constant process temperature throughout the duration of the experiment.

## D. Statistical Design of Experiments

In the conventional procedure for multi-factor experiments, optimization of a process is tedious. It involves carrying out experiments by varying single factor at a time and maintaining the remaining factors as constant. This conventional experimentation procedure is not only time-consuming but also expensive. Another disadvantage with this procedure is that it neglects the interaction between the variables and hence it becomes difficult to determine the true optimum conditions of the process. Design of Experiments, on the other hand, addresses this disadvantage as it involves a planned experimental approach with less number of experiments. Therefore, a properly designed set of experiments in which all factors are chosen and varied systematically will help in determining the factors which have a significant influence on the process response. It also helps in determining the interaction among those factors and finally aids in determining the optimum operating conditions of the specific process. It also generates an empirical expression that may be used in predicting the process response at different factor settings.

TABLE II  
FACTORS AND LEVELS IN EXPERIMENTAL DESIGN

Factor	High level (+1)	Low level (-1)
(A) Initial concentration (IC) (mg/L)	300	100
(B) Stirring speed (RPM)	800	400
(C) Adsorbent loading (g/L)	1.6	0.8
(D) Temperature (T) (°C)	45	25

TABLE III  
EXPERIMENTAL DESIGN IN THE CODED FORM AFTER RANDOMIZATION OF THE SEQUENCE OF EXPERIMENTAL RUNS

Run	Factor A	Factor B	Factor C	Factor D
1	0	0	0	0
2	1	-1	-1	1
3	-1	1	1	1
4	1	1	-1	-1
5	-1	-1	-1	-1
6	-1	1	-1	-1
7	-1	-1	1	1
8	0	0	0	0
9	1	1	1	1
10	-1	1	1	-1
11	1	-1	1	1
12	1	1	1	-1
13	-1	-1	-1	1
14	0	0	0	0
15	-1	1	-1	1
16	-1	-1	1	-1
17	1	1	-1	1
18	1	-1	1	-1
19	1	-1	-1	-1

A full factorial design was employed to design the experiments. The factorial design enables better understanding of the interaction between various parameters. In a two-level full factorial design, each parameter is studied at two levels, viz. at a low level and a high level. In the coded form, a low level is indicated by -1, a high level is indicated by +1 and a

center point is indicated by 0. Coding also helps in removing the effects of units and possibly a wide disparity between the actual values of the factors. A two level full factorial design consists of  $2^k$  number of experiments involving  $k$  factors, with each factor at two levels [3]. Table II shows the factors and the levels involved in the experimental design. Table III shows the coded form of the experimental design. Three center point runs were also performed as repeats in order to determine the error involved in experimentation. % Removal of the dye at equilibrium conditions and  $t_{50}$  (the time required to attain 50% of the eventual equilibrium value at the given temperature) were the chosen responses.

#### E. Adsorption Experiments

Adsorption equilibrium experiments were carried out in an orbital shaker procured from REMI. Three different adsorbent loadings ( $w$ ) were chosen for conducting the experiments, which are 0.8, 1.2 and 1.6 g/L. Similarly, three different initial concentrations of the AO10 dye were chosen, 100, 200 and 300 mg/L. Solutions with initial dye concentrations of 100, 200 and 300 mg/L were prepared in conical flasks. The pH of each solution was adjusted to a uniform value of 4 using 0.1M HCl since adsorption of AO10 is better in acidic conditions [4], [5]. Each flask was then loaded with a particular amount of adsorbent such that each solution had a different combination of initial dye concentration to adsorbent loading. The flasks were then placed in an orbital shaker. Temperature was set to the desired value. The solutions were allowed to equilibrate for five days at 100 RPM in the orbital shaker. The concentration of the solution was checked periodically using Jasco V-730 spectrophotometer. After five days the solutions were removed from the orbital shaker and the concentration of dye solution in each flask was noted. Adsorption capacity of the adsorbent at equilibrium,  $q_e$  (mg/g) was found using (1):

$$q_e = \frac{(C_o - C_e)V}{m_A} \quad (1)$$

The % Removal of AO10 dye at equilibrium was one of the response variables considered in the analysis and is given by (2):

$$\% \text{ Removal} = \frac{(C_o - C_e)}{C_o} \times 100 \quad (2)$$

where,  $C_o$  is the initial concentration of the AO10 sample (mg/L),  $C_e$  is the equilibrium concentration of the AO10 sample (mg/L),  $q_e$  is the amount of AO10 dye adsorbed per gram of adsorbent, at equilibrium (mg/g),  $V$  is the volume of the adsorbate solution (L) and  $m_A$  is adsorbent dosage (g).

Kinetic experiments were carried out in the process vessel mentioned earlier. 500 mL of dye solution of a specific concentration was made; the pH of the solution was changed to 4. The temperature of the solution was adjusted by adjusting the temperature of the water circulated by the constant temperature bath. The stirrer's speed was set to the desired value using the digital RPM controller. Samples were drawn at predetermined intervals of time and analyzed using a

spectrophotometer. From this data the adsorption at time 't' was determined using (3),

$$q_t = \frac{(C_o - C_t)V}{m_A} \quad (3)$$

where,  $C_o$  is the initial concentration of the AO10 sample (mg/L),  $C_t$  is the concentration of the AO10 sample (mg/L) at time 't',  $q_t$  is the amount of AO10 dye adsorbed per gram of adsorbent at time 't',  $V$  is the initial volume of the adsorbate solution (L) and  $m_A$  is adsorbent dosage (g).

Experiments were performed in a randomized fashion as obtained from Design Expert 10.0.0 software (trial version). The experimental runs were randomized in order to avoid systematic error.

#### F. Characterization

The surface imaging studies were conducted using Hitachi S-4800 scanning electron microscopy (SEM). Brunauer-Emmett-Teller (BET) surface analysis was performed using micromeritics ASAP-2020 V4.01. BET surface area  $S_{BET}$  ( $m^2/g$ ), pore volume  $V_T$  ( $cm^3/g$ ) and  $N_2$  adsorption-desorption isotherms were obtained from the BET analysis. The average pore diameter  $D_p$  (m) was calculated using (4) [6]

$$D_p = \frac{4V_T}{S_{BET}} \quad (4)$$

Energy dispersive X-ray analysis (EDX) analysis was performed on the AC before and after the experiment. The EDX analysis revealed information about the elements present in the AC. By performing EDX on the carbon obtained after experimentation it was possible to quantitatively determine the extent of adsorption.

### III. RESULTS AND DISCUSSION

#### A. SEM Analysis

SEM analysis showed a clear picture of the surface of AC. When compared with the image of AC obtained after experimentation, the dye adsorbed on the AC was clearly visible. The pores of the AC were occupied by the particles of the dye. Fig. 2 shows a comparison between fresh AC and AC obtained after the adsorption experiment.

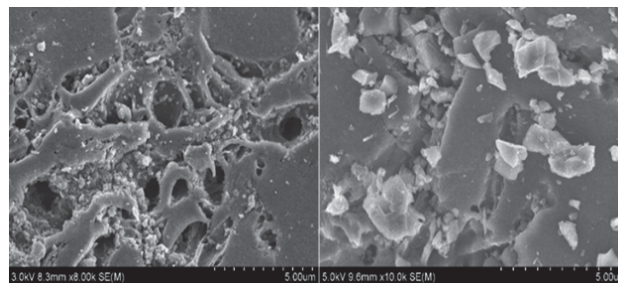


Fig. 2 Comparison between fresh AC (pores are visible) and AC obtained after the experiment

### B. EDX Analysis

The EDX spectrum of fresh AC sample and of the AC sample obtained after the experimentation are shown in Fig. 3. In the fresh sample the main elements present were carbon and a small amount of Oxygen. In the EDX spectrum belonging to the AC obtained after the experiment, a certain quantity of Sulfur was found. This Sulfur was detected as a result of the dye adsorbed on the carbon. The elemental analysis is shown in Table IV.

TABLE IV  
EDX ELEMENTAL ANALYSIS

Element	Weight % before experiment	Weight % after experiment
Carbon	85.84	85.76
Oxygen	14.16	11.85
Sulphur	0.0	2.4

### C. BET Analysis

In order to understand more about the textural characteristic of the AC  $N_2$  adsorption-desorption was performed on the AC at 77K. The adsorption-desorption isotherm obtained is shown in Fig. 4. The isotherm does not show reversibility. The hysteresis loop belongs to type H4 as indicated by IUPAC. In this case the H4 loop has a type I isotherm character which is indicative of micropores [7].

BET analysis was performed on the AC.  $S_{BET}$  was found out to be  $850.438 \text{ m}^2/\text{g}$ . It was observed that the AC was micro porous and the total micro pore volume was reported as  $0.3726 \text{ cm}^3/\text{g}$ . The microporous nature of the AC was also verified by finding out the average pore diameter ( $D_p$ ) of the pores present. The value of  $D_p$  was found out to be  $1.752 \text{ nm}$ , which clearly falls in the micro porous region [7].

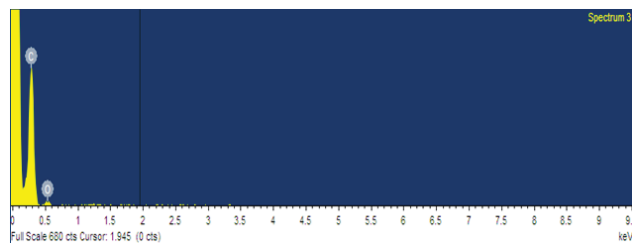


Fig. 3 (a) EDX spectrum of fresh AC

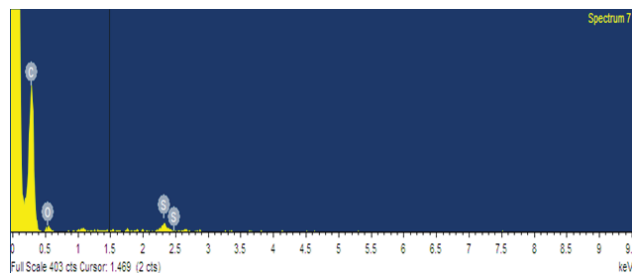


Fig. 3 (b) EDX spectrum of AC obtained after experiment

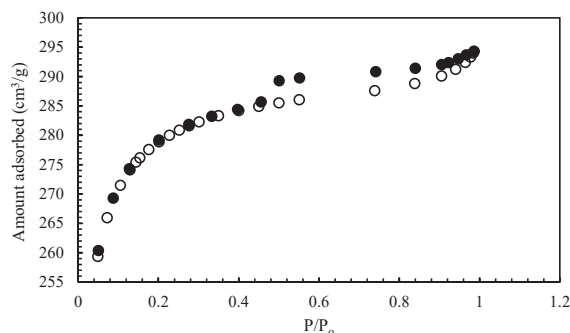


Fig. 4  $N_2$  adsorption ( $\circ$ ) and desorption ( $\bullet$ ) isotherm at 77K

### D. Effect of Initial Concentration

The adsorption of AO10 dye increased with an increase in the initial concentration of the dye. Fig. 5 shows the variation of adsorption capacity with respect to time for different initial concentrations while the remaining factors were held constant. The adsorption process is faster when the initial concentration of the dye solution is higher. This is because of the abundance of dye molecules at higher initial dye concentration and higher concentration driving force. Due to this, the surface of the adsorbent gets saturated quickly as compared to the one where the initial dye concentration is low. The adsorbent capacity at equilibrium was also found to be higher when the initial dye concentration was high. However, the adsorption process becomes slow with time irrespective of the initial concentration. This is because at later stages the adsorption predominantly happens in the pores of the adsorbent which is a slow process [8].

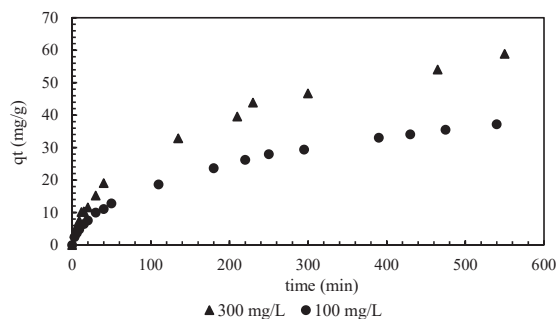


Fig. 5 Comparison of adsorption curves with different initial concentrations

### E. Effect of Stirring Speed

It was found that stirring speed had no effect on the adsorption process for this system. Fig. 6 shows different plots of %Removal vs. Time at different process conditions. In each plot the variation of %Removal of the dye with respect to time is shown for two different stirring speeds (800 RPM & 400 RPM) while all the other factors were held constant. This may be due to the adsorption process being controlled by diffusion alone. This also indicates that the external convective mass transfer resistance is substantially overcome even at 400 rpm and hence stirring at 800 rpm is more energy consuming and practically unnecessary. The increase in mass transfer due to

increased stirring speed does not have any significant effect on the adsorption process.

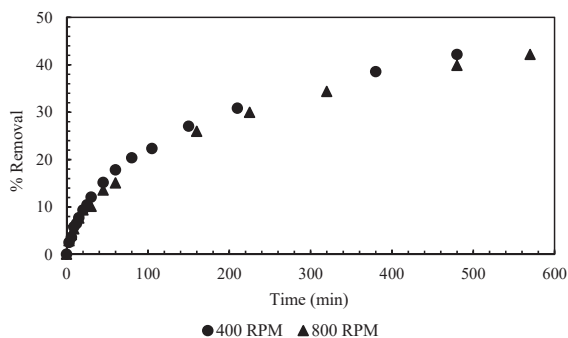


Fig. 6 (a) IC = 100 mg/L; T = 45°C; w = 0.8g/L

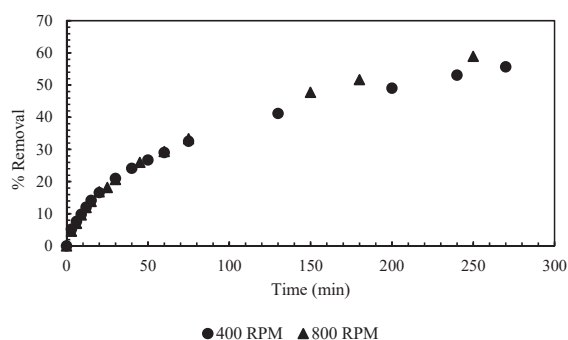


Fig. 6 (b) IC = 100 mg/L; T = 45°C; w = 1.6g/L

#### F. Effect of Temperature

Process temperature had a considerable effect on the adsorption process. Higher temperatures were found to be favorable for the dye adsorption process as observed by some other authors as well [8]–[10]. Increasing the process temperature hastened the adsorption kinetics as shown in Fig. 7. The reason for this behavior may be because of increased mobility of the dye molecules at higher temperatures [8]. This causes the dye molecules to get adsorbed onto the surface of the adsorbent readily. It was observed that the equilibrium adsorption capacity of the adsorbent also increased with an increase in temperature. This has been shown in Fig. 8.

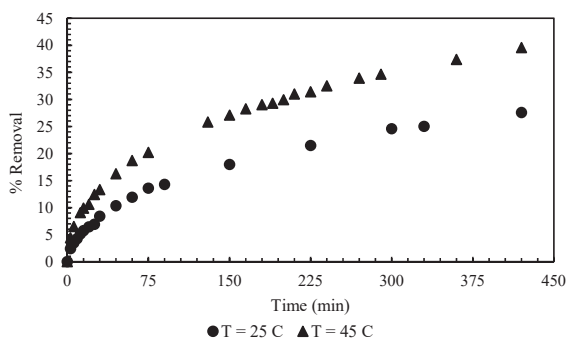


Fig. 7 Adsorption kinetic data at different process temperatures (°C)

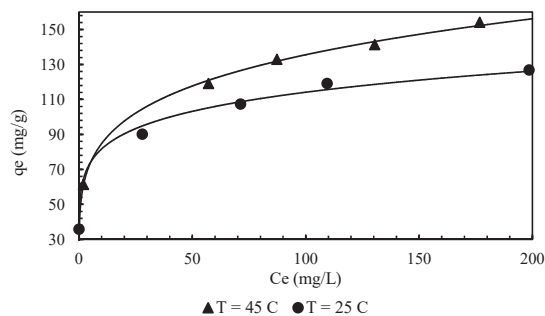


Fig. 8 Adsorption equilibrium data at different process temperatures (in °C)

#### G. Adsorption Isotherms

The Langmuir adsorption isotherm assumes monolayer adsorption on the surface of the adsorbent. The non-linear form of the equation is given by (5).

$$q_e = q_m \frac{k_L C_e}{1 + k_L C_e} \quad (5)$$

where  $q_e$  is the amount of AO10 dye adsorbed at equilibrium (mg/g),  $C_e$  is the amount of AO10 dye present in the solution at equilibrium (mg/L),  $q_m$  and  $k_L$  (Langmuir constants) denote maximum monolayer adsorbent capacity and affinity of adsorbent towards adsorbate respectively.

The adsorption isotherm data obtained at different temperatures was fitted into this model. The model parameters were estimated and the results are shown in Table V. It was observed that the Langmuir adsorption model fitted well with the equilibrium isotherm data obtained. Through the values of  $q_m$  obtained, the model was also able to explain the higher adsorption capacity of the adsorbent at higher temperatures.

The non-linear form of the Freundlich isotherm is given by (6).

$$q_e = k_F C_e^{1/n} \quad (6)$$

where  $q_e$  is the amount of AO10 dye adsorbed at equilibrium (mg/g),  $C_e$  is the amount of AO10 dye present in the solution at equilibrium (mg/L),  $n$  and  $k_F$  are the Freundlich adsorption isotherm coefficients. The value of  $n$  (heterogeneity factor) shows whether the adsorption process is linear ( $n = 1$ ), physical ( $n > 1$ ) or chemical ( $n < 1$ ). Further, a value of  $1/n < 1$  indicates a normal Langmuir isotherm whereas  $1/n > 1$  indicates cooperative adsorption [11].

The adsorption isotherm data obtained was fitted into the Freundlich isotherm model and the model parameters were estimated. The results are shown in Table V. The Freundlich adsorption model fitted the adsorption isotherm data better than the Langmuir model. From Fig. 8, it is clear that the  $q_e$  values are higher at higher temperatures. But in the Freundlich model the parameter  $k_F$  seems to decrease with increase in temperature. This effect is outweighed by the increase in the value of  $1/n$ . So there is a net increase in the value of  $q_e$  at higher temperatures. Because of its  $R^2$  value being very close

to 1 and its ability to give an appropriate validation for the increase in  $q_e$  values with an increase in temperature, the Freundlich model was considered to be the better model to fit the equilibrium adsorption data obtained for this system.

#### H. Adsorption Kinetics

In order to completely understand the AO10 adsorption mechanism, the kinetic data obtained was fitted to different kinetic models namely pseudo-first order and pseudo-second order models.

The non-linear form of the Pseudo-first order kinetic model [12] is given by (7):

$$q_t = q_e(1 - e^{-k_1 t}) \quad (7)$$

where  $q_e$  and  $q_t$  are the amount of AO10 dye adsorbed at equilibrium (mg/g) and at time 't' (min).  $k_1$  ( $\text{min}^{-1}$ ) is the rate constant of the adsorption process. The kinetic data obtained was successfully fitted into the model and the model parameters were estimated. The results are shown in Table VI and Fig. 9 shows the kinetic models fitted to the experimental kinetic data.

The non-linear form of the Pseudo-second order kinetic model [12] is given by (8).

$$q_t = \frac{k_2 q_e^2 t}{(1 + k_2 q_e t)} \quad (8)$$

where  $q_e$  and  $q_t$  are the amount of AO10 dye adsorbed at equilibrium (mg/g) and at time 't' (min).  $k_2$  ( $\text{g/mg} \cdot \text{min}$ ) is the rate constant of the adsorption process. The kinetic data obtained was successfully fitted into the model and the model parameters were estimated. The results are shown in Table VI. The pseudo-second order model fitted the experimental data better than the pseudo-first order model. The values of  $q_e$  predicted by the pseudo-second order model was closer to the experimental value than the one predicted by the pseudo-first order model. A previous study on AO10 adsorption had also concluded along the same lines [13].

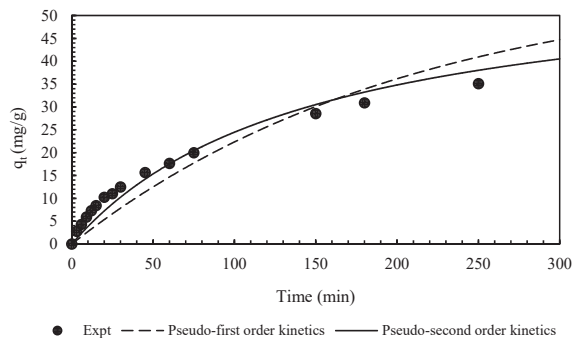


Fig. 9 Kinetic models fitted to experimental kinetic data

#### I. Statistical Optimization

Statistical Optimization was performed using Design Expert 10.0.0 (trial version). The ANOVA (Analysis of Variance) table was made for both the responses namely  $t_{50}$  and % Removal.

##### $t_{50}$ Analysis

The result of the ANOVA analysis made for the response ' $t_{50}$ ' is shown in Table VII.

According to the ANOVA analysis the fitted model had an R-Squared value of 0.919 and an Adjusted R-Squared value of 0.838. From the ANOVA analysis it was observed that A, C, D and CD were the significant model terms. The equation of the fitted model is given below

$$t_{50} = 429.579 + 44.125 * A - 13 * B - 93.5 * C - 111.625 * D + 35.5 * AC - 6.125 * AD + 15 * BD + 37.25 * CD - 1 * ACD$$

It may be seen that the above equation includes all the factors and their interactions. However, inspection of the equation shows that some coefficients are insignificant relative to the others. Using the p-values in the ANOVA table and considering terms that have p-values  $> 0.05$ , to be insignificant, we reduce the above model equation to

$$t_{50} = 429.579 + 44.125 * A - 93.5 * C - 111.625 * D + 37.25 * CD$$

TABLE V  
ADSORPTION ISOTHERM MODEL PARAMETERS

Temperature (°C)	Langmuir parameters			Freundlich parameters		
	$q_{\max}$ (mg/g)	$k_L$ (L/mg)	$R^2$	$k_F$ (mg/g)(L/mg) <sup>1/n</sup>	1/n	$R^2$
25	110.9	23.61	0.94	58.48	0.145	0.995
45	141	0.379	0.97	53.01	0.203	0.999

TABLE I  
KINETIC MODEL PARAMETERS

IC (mg/L)	Temperature (°C)	$q_{\text{exp}}$ (mg/g)	Pseudo-first order parameters			Pseudo-second order Parameters		
			$k_1$ ( $\text{min}^{-1}$ )	$q_{e, \text{cal}}$ (mg/g)	$R^2$	$K_2$ (g/mg.min) x 10 <sup>-4</sup>	$q_{e, \text{cal}}$ (mg/g)	$R^2$
100	25	60.54	0.0025	56.63	0.937	0.615	59.27	0.974
300		119.13	0.0014	113.2	0.929	0.168	119.9	0.961
100	45	61.31	0.0048	58.59	0.944	1.13	60.25	0.98
300		132.97	0.0058	99.3	0.895	5.58	115.8	0.954

TABLE II  
ANOVA TABLE FOR  $t_{50}$  ANALYSIS

Source	Sum of Squares	Mean Square	F Value	p-value	Significance
				Prob > F	
Model	419675.8	46630.64	11.38231	0.000631	<b>Significant</b>
A-Initial concentration	31152.25	31152.25	7.60411	0.022201	<b>Significant</b>
B-Stirrer speed	2704	2704	0.660033	0.437509	Insignificant
C-Adsorbent loading	139876	139876	34.14304	0.000246	<b>Significant</b>
D-Temperature	199362.3	199362.3	48.66334	6.5E-05	<b>Significant</b>
AC	20164	20164	4.921933	0.053692	Insignificant
AD	600.25	600.25	0.146518	0.710769	Insignificant
BD	3600	3600	0.878742	0.373019	Insignificant
CD	22201	22201	5.419154	0.044901	<b>Significant</b>
ACD	16	16	0.003906	0.951535	Insignificant
Residual	36870.88	4096.765			
Lack of Fit	36312.88	5187.555	18.59339	0.051974	Insignificant
Pure Error	558	279			
Total	456546.6				

Stirrer speed, at the factor settings investigated, is insignificant. The adsorbent loading and temperature factors are significant.

#### % Removal Analysis

The result of the ANOVA analysis made for the response '% Removal' is shown in Table VIII.

According to the ANOVA analysis the fitted model had an R-Squared value of 0.99 and an Adjusted R-Squared value of 0.982. From the ANOVA analysis it was also found out that

A, C, D and AD were the significant model terms. The equation of the fitted model is given below in terms of significant factors and interactions.

$$\% \text{ Removal} = 69.5584 - 16.3631 * A + 13.6481 * C + 2.12563 * D + 1.53812 * AD$$

Numerical optimization was performed for maximizing % removal and minimizing  $t_{50}$ . The conditions obtained are given in Table IX.

TABLE VIII  
ANOVA TABLE FOR %REMOVAL ANALYSIS

Source	Sum of Squares	Mean Square	F Value	p-value	Significance
				Prob > F	
Model	7398.96	924.87	123.68	< 0.0001	<b>significant</b>
A-Initial concentration	4284.03	4284.03	572.88	< 0.0001	<b>significant</b>
B-Stirrer speed	5.63E-05	5.63E-05	7.52E-06	0.9979	Insignificant
C-Adsorbent loading	2980.34	2980.34	398.55	< 0.0001	<b>significant</b>
D-Temperature	72.29	72.29	9.67	0.0111	<b>significant</b>
AC	24.43	24.43	3.27	0.1008	Insignificant
AD	37.85	37.85	5.06	0.0482	<b>significant</b>
CD	0.012	0.012	1.55E-03	0.9694	Insignificant
ACD	6.25E-06	6.25E-06	8.36E-07	0.9993	Insignificant
Residual	74.78	7.48			
Lack of Fit	74.78	9.35			Insignificant
Pure Error	0	0			
Total	7473.74				

TABLE IX  
OPTIMIZED CONDITIONS

Condition	Initial Concentration (mg/L)	Stirrer Speed (rpm)	Adsorbent Loading (g/L)	Temperature (°C)	$t_{50}$ (min)	% Removal (%)
Maximizing % Removal	100.13	469.76	1.6	44.64	288	98.12
Minimizing $t_{50}$	100	400	1.6	45	187	98.95
Maximizing % Removal and minimizing $t_{50}$	100	400	1.6	45	187	98.95

The last condition was considered as the most suitable optimal condition. Experiments were performed for the above condition and the  $t_{50}$  was obtained at 194 minutes and a percentage removal of 98.09%.

#### IV. CONCLUSION

Adsorption of the hazardous AO10 dye on activated carbon was investigated. The AC was characterized using SEM, BET and XRD. The results obtained from various characterization

techniques was studied and it was found that the AC was predominantly micro-porous. A full factorial design was used to systematically analyze the effect that various process conditions (Initial concentration, temperature, stirring speed and adsorbent loading) have on the adsorption process.

The experimental data was fitted to different adsorption isotherm as well as kinetic models. Freundlich adsorption isotherm was found to be the suitable isotherm model and a pseudo-second order model was able to give a reasonable fit for the kinetic data. It was found that initial dye concentration, adsorbent loading and temperature had the greatest effect on the adsorption process. An increase in the magnitude of any of these parameters enhanced the adsorption process. Statistical optimization was performed to identify optimal condition at which the dye removal is high as well as rapid. The resulting condition was validated experimentally.

#### REFERENCES

- [1] J. J. Gooding, R. G. Compton, C. M. Brennan, and J. H. Atherton, "The mechanism of the electro-reduction of some azo dyes," *Electroanalysis*, vol. 8, pp. 4–8, 1996.
- [2] K. Ramakrishna and T. Viraraghavan, "Dye removal using low cost adsorbents," *Water Sci. Technol.*, vol. 36, no. 2–3, pp. 189–196, 1997.
- [3] D. Bingol, N. Tekin, and M. Alkan, "Brilliant Yellow dye adsorption onto sepiolite using a full factorial design," *Appl. Clay Sci.*, vol. 50, no. 3, pp. 315–321, Nov. 2010.
- [4] I. D. Mall, V. C. Srivastava, and N. K. Agarwal, "Removal of Orange-G and Methyl Violet dyes by adsorption onto bagasse fly ash d kinetic study and equilibrium isotherm analyses," vol. 69, pp. 210–223, 2006.
- [5] A. A. Atia, A. M. Donia, and W. A. Al-Amrani, "Adsorption/desorption behavior of acid orange 10 on magnetic silica modified with amine groups," *Chem. Eng. J.*, vol. 150, no. 1, pp. 55–62, 2009.
- [6] A. C. Martins, O. Pezoti, A. L. Cazetta, K. C. Bedin, D. A. S. Yamazaki, G. F. G. Bandoch, T. Asefa, J. V. Visentainer, and V. C. Almeida, "Removal of tetracycline by NaOH-activated carbon produced from macadamia nut shells: Kinetic and equilibrium studies," *Chem. Eng. J.*, vol. 260, pp. 291–299, 2015.
- [7] K. S. W. Sing, D. H. Everett, R. A. W. Haul, L. Moscou, R. A. Pierotti, J. Rouquerol, and T. Siemieniewska, "International Union of Pure Commission on Colloid and Surface Chemistry Including Catalysis" Reporting Physisorption Data for Gas / Solid Systems with Special Reference to the Determination of Surface Area and Porosity," *Pure Appl. Chem.*, vol. 54, no. 11, pp. 2201–2218, 1982.
- [8] B. H. Hameed, A. A. Ahmad, and N. Aziz, "Isotherms, kinetics and thermodynamics of acid dye adsorption on activated palm ash," *Chem. Eng. J.*, vol. 133, no. 1–3, pp. 195–203, 2007.
- [9] A. Rodriguez, J. Garcia, G. Ovejero, and M. Mestanza, "Adsorption of anionic and cationic dyes on activated carbon from aqueous solutions: Equilibrium and kinetics," *J. Hazard. Mater.*, vol. 172, no. 2–3, pp. 1311–1320, 2009.
- [10] I. A. W. Tan, A. L. Ahmad, and B. H. Hameed, "Enhancement of basic dye adsorption uptake from aqueous solutions using chemically modified oil palm shell activated carbon," *Colloids Surfaces A Physicochem. Eng. Asp.*, vol. 318, no. 1–3, pp. 88–96, 2008.
- [11] A. L. Cazetta, A. M. M. Vargas, E. M. Nogami, M. H. Kunita, M. R. Guilherme, A. C. Martins, T. L. Silva, J. C. G. Moraes, and V. C. Almeida, "NaOH-activated carbon of high surface area produced from coconut shell: Kinetics and equilibrium studies from the methylene blue adsorption," *Chem. Eng. J.*, vol. 174, no. 1, pp. 117–125, 2011.
- [12] M. Auta and B. H. Hameed, "Preparation of waste tea activated carbon using potassium acetate as an activating agent for adsorption of Acid Blue 25 dye," *Chem. Eng. J.*, vol. 171, no. 2, pp. 502–509, Jul. 2011.
- [13] M. Arulkumar, P. Sathishkumar, and T. Palvannan, "Optimization of Orange G dye adsorption by activated carbon of *Thespesia populnea* pods using response surface methodology," *J. Hazard. Mater.*, vol. 186, no. 1, pp. 827–834, 2011.